ILASS–Europe 2017, 28th Conference on Liquid Atomization and Spray Systems, 6-8 September 2017, Valencia, Spain
http://dx.doi.org/10.4995/ILASS2017.2017.4615

Analytical / Computational Approach to Liquid Spray Heating and Vaporization at Supercritical Pressures

Albert Jordà Juanós[1] and William A. Sirignano*,[1]
[1]Department of Mechanical and Aerospase Engineering, University of California, Irvine, CA 92697-3975, U.S.A.
*Corresponding author: sirignan@uci.edu

Abstract
Our findings from two areas of background research will define an approach to the study of liquid spray heating and vaporization in gases at supercritical pressure: (i) vaporizing droplets at supercritical pressure and (ii) supercritical combustion in simple configurations, e.g., counterflow. The a priori conclusion that only one phase exists at supercritical pressure is based on false "lore" and not physical law. The question about the phases must be left open until the analysis reaches a conclusion; a proper approach will be defined. Proper equations of state for density and enthalpy and the determination of phase equilibrium, liquid composition due to dissolved gas, energy of vaporization, surface tension, and transport properties for high pressures will be discussed. The case of an isolated droplet will be reviewed and origin of the transcritical concept will be explained. A counterflow spray configuration at pressures above the liquid critical pressure will be analyzed. The concept of shifting phase equilibrium will be applied as the droplets in the spray heat. Hydrocarbon liquids and oxidizing gaseous environments will be studied. Differences between real fluids and ideal fluids at high pressures will be emphasized. Proper rules for gaseous mixtures and liquid solutions will be discussed.

Keywords
High pressure, supercritical, phase equilibrium.

Introduction

Combustion of hydrocarbons at high pressure is becoming more important in a broad range of engineering applications, such as diesel engines, gas turbines, and rocket engines, where fuels are usually in liquid phase. There are several issues related to these situations that are not mastered in the combustion literature and must be addressed. (1) The critical pressure of a mixture is commonly substantially higher than the critical pressure of any component. Thus, two phases can easily exist at so-called "supercritical" conditions. (2) Since critical pressure varies with composition, a volume (even at uniform pressure and temperature) can have subcritical portions and supercritical portions in space and/ or time. (3) At subcritical mixture conditions, large amounts of ambient gas will dissolve in the fluid and diffuse away from the liquid-gas interface into the liquid interior. Thus, an injected liquid cannot be assumed to have its original composition or any uniform composition; its density, surface tension, specific heat, and transport properties can change with time and space. (4) Consequently, because of density gradients on both sides of the interface, an experimental image showing a fuzzy interface cannot be sufficient proof of single-phase behavior. (5) Even at true supercritical conditions, there can be a pseudo-two-phase behavior. A narrow domain can exist in temperature-pressure space across which sharp changes in density and can occur. Although the changes are not discontinuous like the true two-phase case, there can be similar consequences. (6) Transport rates decrease and chemical rates increase with increasing pressure. Therefore, the rate-controlling mechanism can change. In the presentation, most of these issues will be discussed. They are not all addressed herein.

In real application combustors, the fuel often enters the combustion chamber at sub-critical temperatures but supercritical pressures, resulting in a "trans-critical" situation [1]. While droplets can be immersed in a gas, the situation is not simply traditional non-premixed combustion. The ambient hot fluid is supercritical but the cold liquid is not supercritical although existing at supercritical pressure. The gaseous mixture in the film neighboring can have a higher critical pressure than any component of the mixture. So, the mixture critical pressure can vary significantly both spatially and temporally. For the same nearly uniform pressure and at the same instant, there can be fluid regions at sub-critical conditions and other regions that are supercritical.

Liquid-vapor phase equilibrium calculations have been used in the past for applications primarily related to the oil and refinery industries. Less attention has been given to situations where liquid-fuel injection is used. Analysis of length- and time-scales associated to the a liquid jet indicates that diffusion of species from the surrounding fluid into the liquid jet occurs much faster than the break-up process of the liquid, and the diffusion layer is much greater than the molecular spacing, even at very high pressures. Thus, continuum theory must be applied in such region with the proper evaluation of thermodynamic properties for a gaseous mixture and liquid solution. The first approach in the analysis of such situations is the study of vapor-liquid equilibrium at high pressure. Results are presented in the next section both for binary mixtures and for mixtures with more than two components. The following section presents the model that accounts for variations in the system composition and temperature due to heat addition.

This work is licensed under a Creative Commons 4.0 International License (CC BY-NC-ND 4.0).
EDITORIAL UNIVERSITAT POLITÈCNICA DE VALÈNCIA

High-Pressure Phase Equilibrium

The formulation for high-pressure phase equilibrium is well known and can be found in several thermodynamic and chemical engineering books (i.e. [2, 3]). Qualitative behavior of mixture critical pressure and temperature was also described in these and other references. The main novelty in our results is in the evaluation of the SRK EOS for particular hydrocarbon-oxygen mixtures as well as the methane-water mixture. The formulation is reviewed below, and results of interest for current combustion mixtures are included.

Thermal, mechanical and chemical potential must be balanced between the liquid and the gas phases for a multi-component mixture to be in equilibrium:

$$T^{\ell} = T^{\prime\prime} \quad ; \quad P^{\ell} = P^{\prime\prime} \quad ; \quad \mu^{\ell} = \mu^{\prime\prime} \tag{1}$$

The relationship between chemical potential and fugacity is:

$$\mu_i^{\diamond} - \mu_i = R_u T \ln \frac{f_i}{f_i^{\diamond}} \quad \text{and} \quad \lim_{P \to 0} \left(\frac{f_i}{P_i} \right) \to 1 \tag{2}$$

The chemical potential equality may be expressed in terms of the fugacity as $f_i^{\ell} = f_i^{\prime\prime}$, whereby, bringing in the fugacity coefficient gives

$$\chi_i^{\ell} \phi_i^{\ell} = \chi_i^{\prime\prime} \phi_i^{\prime\prime} \quad \text{where} \quad \sum_{i=1}^{N} X_i^{\ell} = 1, \; \sum_{i=1}^{N} X_i^{\prime\prime} = 1 \tag{3}$$

For systems with only two species, Equations 3 are used to solve for the mole fractions of each species in both liquid and gas phases. A dedicated code has been written to obtain solutions. Iterations are performed using the "fsolve" Matlab function until convergence is achieved.

The Soave-Redlich-Kwong Equation of State (SRK EoS) is selected because of its reasonable accuracy for a wide range of fluid states [4]. It is presented below both in its original form and in its cubic form in terms of compressibility factor Z. In the following, p, T, R_u, and $\overline{v}$ stand for pressure, temperature, universal gas constant, and molar specific volume, respectively.

$$p = \frac{R_u T}{\overline{v} - b} - \frac{a}{\overline{v}(\overline{v} + b)}; \quad Z^3 - Z^2 + (A - B - B^2)Z - AB = 0; \quad Z \equiv \frac{p\overline{v}}{R_u T}; \quad A \equiv \frac{ap}{(R_u T)^2}; \quad B \equiv \frac{bp}{R_u T} \tag{4}$$

This empirical equation has two parameters a and b, which are constants for single-component fluids, but become composition, pressure, and temperature dependent in the multicomponent version. The parameter mixing rules of the Soave-Redlich-Kwong EoS are employed [5]:

$$a = \sum_{i=1}^{K} \sum_{j=1}^{K} X_i X_j (a_i a_j)^{0.5} (1 - k_{ij}) \quad ; \quad b = \sum_{i=1}^{K} X_i b_i \tag{5}$$

The pure species attractive and repulsive parameters a_i and b_i may be obtained from the species critical points as

$$\begin{aligned} &a_i = a_{ci} \alpha_i \;\; ; \;\; a_{ci} = 0.42748 \frac{(R_u T_{ci})^2}{P_{ci}} \;\; ; \;\; \alpha_i^{0.5} = 1 + S_i (1 - T_{ri}^{0.5}) \\ &S_i = 0.48508 + 1.5517 \omega_i - 0.15613 \omega_i^2 \;\; ; \;\; b_i = 0.08664 \frac{R_u T_{ci}}{P_{ci}} \end{aligned} \tag{6}$$

where T_{ci} and P_{ci} are the critical temperature and critical pressure of mixture component i, k_{ij} is the characteristic binary interaction constant and ω_i are the acentric factors. These values are taken from the literature [6]. Sub-index r stands for "reduced" and equals the property temperature or pressure divided by its critical value.

Note that the mixing rules are associated to each equation of state. Binary interaction coefficients $k_i j$ are also dependent on the chosen equation of state, and they can be found in the literature, at least for the major species.

From basic thermodynamic relations, the fugacity coefficient can be expressed in terms of temperature and volume (or temperature and pressure). For the SRK EoS case, the fugacity coefficient of species i is

$$ln[\Phi_i] = \frac{b_i}{b}(Z - 1) - ln[Z - B] - \frac{A}{B}\left(2\left(\frac{a_i}{a}\right)^{0.5} - \frac{b_i}{b}\right) ln\left[1 + \frac{B}{Z}\right] \tag{7}$$

The specific enthalpy departure function for the SRK EoS is given by [7]:

$$h - h^* = \frac{1}{\overline{W}} \left[R_u T (Z - 1) + \frac{T \frac{da}{dT} - a}{b} ln \frac{Z + B}{Z} \right] \tag{8}$$

where h^* is the enthalpy for an ideal gas at the given temperature.

At high pressure values and a given temperature, the energy required to vaporize one mole of component i from the liquid mixture to the gaseous mixture is substantially different from the latent heat of vaporization. The former is the enthalpy of vaporization of component i while the latter is defined as the energy required to vaporize one mole

This work is licensed under a Creative Commons 4.0 International License (CC BY-NC-ND 4.0).
EDITORIAL UNIVERSITAT POLITÈCNICA DE VALÈNCIA

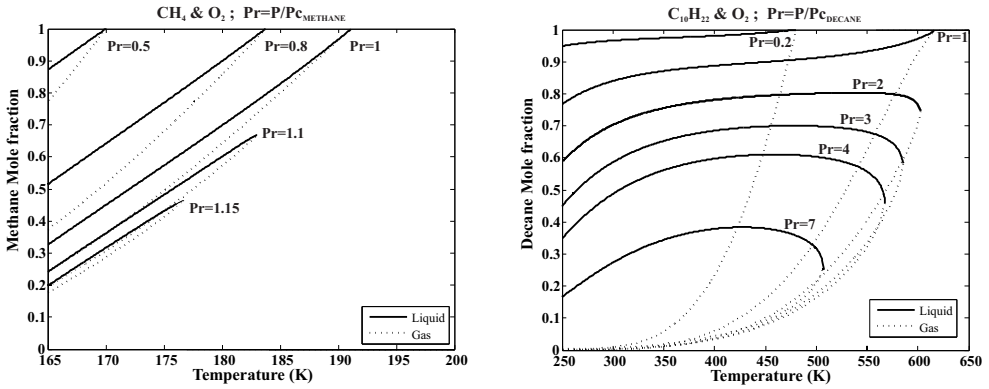

(a) Methane (b) Decane

Figure 1. Binary Systems of (a) methane and oxygen, (b) decane and oxygen, in phase equilibrium (normalizing pressure corresponds to fuel).

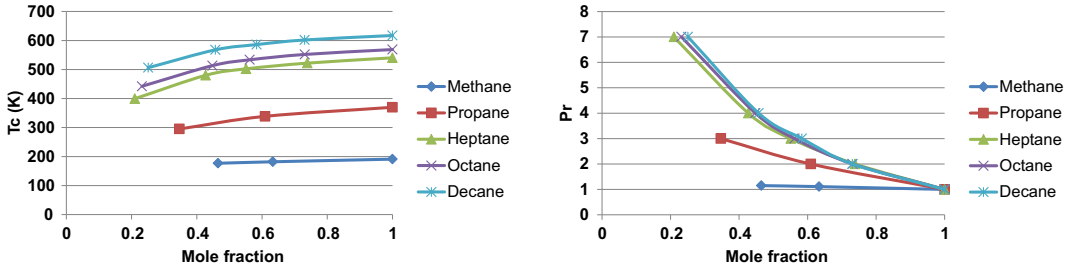

(a) Critical Temperature (b) Reduced Pressure

Figure 2. Critical properties of hydrocarbon/oxygen mixtures vs. mole fraction.

of pure liquid i in its own vapor at a given temperature and the corresponding saturation pressure. The enthalpy of vaporization as a function of the fugacity coefficient is:

$$\Delta\overline{h}_{v,i} = \overline{h}_i^{\mathscr{v}} - \overline{h}_i^{\ell} = R_u T^2 \frac{\partial}{\partial T}\left[\ln\frac{\phi_i^{\mathscr{v}}}{\phi_i^{\ell}}\right] \tag{9}$$

The surface tension coefficient of the liquid σ_i is evaluated using the Parachor parameter for each species P_i, which is taken from the literature [8]:

$$\sigma_i = \left(\frac{P_i}{\overline{v}}\right)^4 \tag{10}$$

where $\overline{v}$ is the molar specific volume given by the EoS.

Two Species

Contrary to most of the hydrocarbons, methane has critical pressure and temperature that are much closer to the critical values for oxygen. Thus, the mixture of these two components are described by curves that are sharper, and the range of pressures for which two phases are obtained is narrower. This effect can be seen in Figure 1a. For a prescribed temperature, increasing the pressure reduces the liquid mole fraction of methane, implying that there is more oxygen being dissolved into the liquid mixture. The oxygen mole fraction in the liquid decreases when the temperature is increased at a given pressure. As heavier hydrocarbons are computed, the differences between the critical properties of the hydrocarbon and the oxygen become greater and the mole fractions of liquid and gas phases are more unequal. This effect may be seen in Figure 1b. For pressures greater than the critical pressure of the hydrocarbon, increasing temperature at a fixed pressure raises the mole fraction of the hydrocarbon in the liquid. However, as the critical pressure is approached, the mole fraction slightly drops again.

The mixture critical temperature values vary monotonically between the maximum and the minimum critical temperature of the two pure species (see Figure 2a). The critical pressure, however, rises higher than the critical pressure of any component species and there can still be two phases (or sub-critical conditions; see Figure 2b). In this last plot, the normalizing pressure for each hydrocarbon is the critical pressure of the pure hydrocarbon. At temperatures below 550 K the methane gaseous phase and the water liquid phase are dominant for all pressures equal or above the critical pressure of water. For temperatures above 550 K, gaseous-water mole fraction increases above 50%. Liquid-water mole fraction is still much greater than liquid methane, with more methane dissolving into the liquid.

This work is licensed under a Creative Commons 4.0 International License (CC BY-NC-ND 4.0).
EDITORIAL UNIVERSITAT POLITÈCNICA DE VALÈNCIA

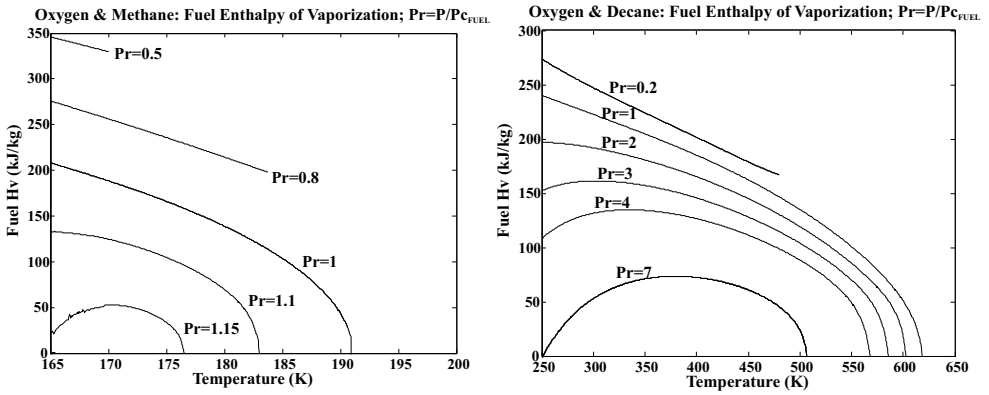

(a) Methane (b) Decane

Figure 3. Hydrocarbon Fuel and Oxygen Enthalpy of Vaporization (Normalizing pressure corresponds to Fuel).

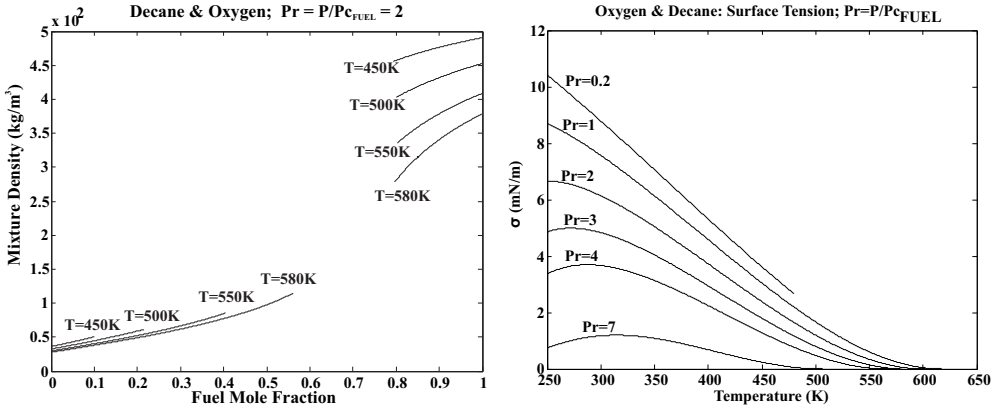

(a) Density vs. Composition (b) Surface Tension

Figure 4. Decane and Oxygen: Density and Surface Tension.

The variation of the enthalpy of vaporization with temperature and pressure is given in Figure 3 for methane, or decane, with oxygen. The enthalpy of vaporization decreases with pressure at constant temperature. At constant pressure, however, the enthalpy of vaporization may increase at low temperatures and then decrease monotonically until it reaches 0 at the critical point.

Figure 4 shows density and surface tension variations for decane with oxygen. In Figure 4a the composition is varied from the liquid/gas phase equilibrium values at prescribed pressure and temperatures. Density increases with increasing decane fraction both for the liquid and for the gas phases. Density increases faster in the liquid than in the gas with increasing fuel fraction. Figure 4b shows how surface tension tends to decrease with temperature at constant pressure until it reaches 0 at the critical point. However, surface tension increases with temperature at low temperature ranges and high pressures. At constant temperature, surface tension decreases with increasing pressure.

Four Species

Analysis of phase-equilibrium for a mixture composed of reactants and products is of interest for applications such as Exhaust Gas Recirculation (EGR). A single-step stoichiometric reaction between decane and oxygen results in mixtures with four major species: $C_{10}H_{22}$, O_2, H_2O, and CO_2. Two mole fraction ratios must be constrained to conduct the phase equilibrium calculation. We will consider CO_2 and H_2O predominantly in the gas phase and always in the product stoichiometric molar proportion of 11/10. The other ratio is selected to be between the oxygen and the products, and will be varied as a parameter. See Figure 5, which applies at twice the critical pressure of the decane, and every curve belongs to one of the oxygen-to-products ratio. As expected, for the higher proportions of oxygen vs. products, concentrations of the reactants are greater in the liquid phase while concentration of products is lower. As temperature is increased, more decane is dissolved into the liquid and less of the other species. For a pure concentration of decane, we get its critical temperature. For low temperatures, more water is in the liquid phase. As temperature is increased, the fraction of water in either phase decreases. The same occurs for oxygen and carbon dioxide, although these two are predominantly in the gas phase. For pressures greater than the critical pressure of decane, altering the ratio between oxygen and products changes the critical temperature of the mixture. Ratios with more oxygen weight result in higher critical temperatures. As it happened for the decane-oxygen binary system, decane mole fraction decreases for a pressure increment. Liquid oxygen mole fraction, however, increases. The fraction of oxygen that dissolves into the liquid increases with increasing pressure and also with increasing

This work is licensed under a Creative Commons 4.0 International License (CC BY-NC-ND 4.0).
EDITORIAL UNIVERSITAT POLITÈCNICA DE VALÈNCIA

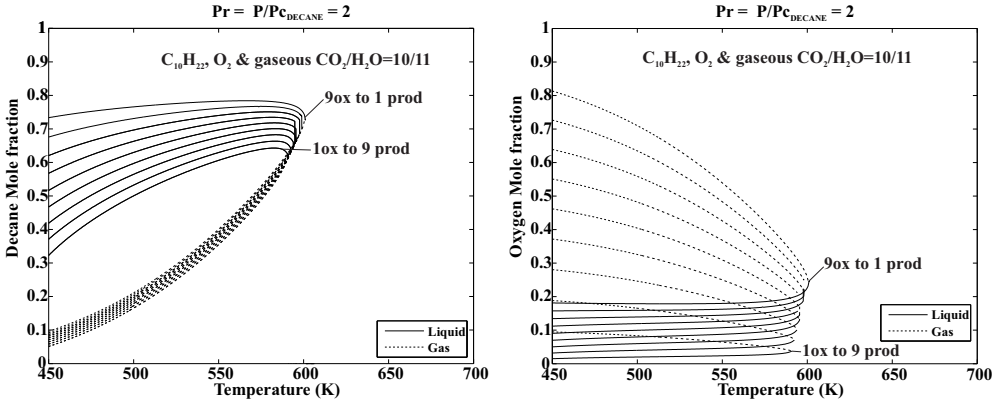

(a) Decane Mole Fraction (b) Oxygen Mole Fraction

Figure 5. Decane, Oxygen and Products Phase Equilibrium ($P_r = P/P_{c_{DECANE}} = 2$).

oxygen-to-product ratio. The same effect occurs with CO_2.

Two-Phase Shifting Equilibrium

High-pressure phase equilibrium was described in the previous section and solutions for different binary and multicomponent mixtures were reported. Here, we analyze the case where a shift in the species mass fractions and density is caused by a temperature change. The latter may be due to heat transferred from combustion in the gas phase occurring in the vicinity of the phase-change location.

With only phase change and no chemical change, N_i (the number of moles of species i) remains fixed at its initial value N_{i0}; that is $N_{gi} + N_{li} = N_i = N_{i0} = constant$. Defining the mole number of the gas mixture as $N_g = \sum_{i=1}^{K} N_{gi}$ and the mole number of the liquid mixture as $N_l = \sum_{i=1}^{K} N_{li}$, where K is the total number of species, we also have $N_g + N_l = N = N_0 = constant$. With this, it is convenient to express the mole fractions normalized over both phases. Let $\xi_g \equiv N_g/N_0$; $\xi_l \equiv N_l/N_0$; $\xi_{gi} \equiv N_{gi}/N_0$; and $\xi_{li} \equiv N_{li}/N_0$. Their relation with the common mole fractions are

$$\xi_{gi} = X_{gi}N_g/N_0 = X_{gi}\xi_g;\ \xi_{li} = X_{li}N_l/N_0 = X_{li}\xi_l;\ X_{gi} = \xi_{gi}/\xi_g;\ X_{li} = \xi_{li}/\xi_l;\ i = 1, ..., K-1 \tag{11}$$

Consequently,

$$\xi_{gi} + \xi_{li} = \frac{N_{i0}}{N_0} = \xi_i = \xi_{i0};\ i = 1, ..., K \tag{12}$$

The relations for phase equilibrium were presented in the previous section (see Equation 3). There are K species and K phase-equilibrium relations. Taking changes in Equation 3 due to pressure and temperature, we obtain

$$\begin{aligned}&\left[\Phi_{gi} + X_{gi}\frac{\partial\Phi_{gi}}{\partial X_{gi}}\right]dX_{gi} - \left[\Phi_{li} + X_{li}\frac{\partial\Phi_{li}}{\partial X_{li}}\right]dX_{li} + X_{gi}\left(\sum_{j\neq i}\frac{\partial\Phi_{gi}}{\partial X_{gj}}\right)dX_{gj} - X_{li}\left(\sum_{j\neq i}\frac{\partial\Phi_{li}}{\partial X_{lj}}\right)dX_{lj}\\ &= \left[X_{li}\frac{\partial\Phi_{li}}{\partial p} - X_{gi}\frac{\partial\Phi_{gi}}{\partial p}\right]dp + \left[X_{li}\frac{\partial\Phi_{li}}{\partial T} - X_{gi}\frac{\partial\Phi_{gi}}{\partial T}\right]dT;\ i = 1, ..., K\end{aligned} \tag{13}$$

In a phase change without chemical reaction, we have $\Delta N = 0$; $dN_l = -dN_g$; $d\xi_l = -d\xi_g$; $dN_{li} = -dN_{gi}$; and $d\xi_{li} = -d\xi_{gi}$. It follows that, for small changes in composition due to vaporization or condensation,

$$dX_{li} = \frac{1}{\xi_l}d\xi_{li} - \frac{\xi_{li}}{\xi_l^2}d\xi_l = -\frac{1}{\xi_l}d\xi_{gi} + \frac{\xi_{li}}{\xi_l^2}d\xi_g \quad ; \quad dX_{gi} = \frac{1}{\xi_g}d\xi_{gi} - \frac{\xi_{gi}}{\xi_g^2}d\xi_g;\ i = 1, ..., K \tag{14}$$

Substitution of Equation 14 into Equation 13 yields

$$\beta_{ii}d\xi_{gi} + \sum_{k\neq i}\beta_{ik}d\xi_{gk} = \delta_i dp + \epsilon_i dT;\ i = 1, ..., K \tag{15}$$

where the following definitions are made:

$$\begin{aligned}\beta_{ii} \equiv&\tfrac{\Phi_{gi}}{\xi_g} + \tfrac{\Phi_{li}}{\xi_l} + \tfrac{X_{gi}}{\xi_g}\tfrac{\partial\Phi_{gi}}{\partial X_{gi}} + \tfrac{X_{li}}{\xi_l}\tfrac{\partial\Phi_{li}}{\partial X_{li}} - \tfrac{\Phi_{gi}X_{gi}}{\xi_g} - \tfrac{\Phi_{li}X_{li}}{\xi_l} - \tfrac{X_{gi}}{\xi_g}(\textstyle\sum_{j=1}^{K} X_{gj}\tfrac{\partial\Phi_{gi}}{\partial X_{gi}}) - \tfrac{X_{li}}{\xi_l}(\textstyle\sum_{j=1}^{K} X_{lj}\tfrac{\partial\Phi_{li}}{\partial X_{li}});\\ \beta_{ik} \equiv&\tfrac{X_{gi}}{\xi_g}\tfrac{\partial\Phi_{gi}}{\partial X_{gi}} + \tfrac{X_{li}}{\xi_l}\tfrac{\partial\Phi_{li}}{\partial X_{li}} - \gamma_i\ ,\ k \neq i;\\ \gamma_i \equiv&\tfrac{\Phi_{gi}X_{gi}}{\xi_g} + \tfrac{\Phi_{li}X_{li}}{\xi_l} + \tfrac{X_{gi}}{\xi_g}(\textstyle\sum_{j=1}^{K} X_{gj}\tfrac{\partial\Phi_{gi}}{\partial X_{gi}}) + \tfrac{X_{li}}{\xi_l}(\textstyle\sum_{j=1}^{K} X_{lj}\tfrac{\partial\Phi_{li}}{\partial X_{li}});\\ \delta_i \equiv&X_{li}\tfrac{\partial\Phi_{li}}{\partial p} - X_{gi}\tfrac{\partial\Phi_{gi}}{\partial p};\ \epsilon_i \equiv X_{li}\tfrac{\partial\Phi_{li}}{\partial T} - X_{gi}\tfrac{\partial\Phi_{gi}}{\partial T}; i = 1, ..., K;\ k = 1, ..., i-1, i+1, ..., K\end{aligned} \tag{16}$$

This work is licensed under a Creative Commons 4.0 International License (CC BY-NC-ND 4.0).

Equation 15 presents a linear system of K equations for the K values of $d\xi_g$. It can be solved to yield the solutions. We define $A_i \equiv [\beta_{ik}]^{-1}[\delta_k]$ and $B_i \equiv [\beta_{ik}]^{-1}[\epsilon_k]$:

$$\begin{aligned} d\xi_{gi} &= -d\xi_{li} = A_i dp + B_i dT; \\ dX_{li} &= [\frac{X_{li}\sum_{j=1}^{K} A_j - A_i}{\xi_l}]dp + [\frac{X_{li}\sum_{j=1}^{K} B_j - B_i}{\xi_l}]dT; \\ dX_{gi} &= [\frac{A_i - X_{gi}\sum_{j=1}^{K} A_j}{\xi_g}]dp + [\frac{B_i - X_{gi}\sum_{j=1}^{K} B_j}{\xi_g}]dT; \quad i = 1, ..., K \end{aligned} \tag{17}$$

Assume a small amount of heat per unit mole δq is added to the mixture at constant pressure. As equilibrium shifts, we have

$$d\psi_g = -d\psi_l; \quad d\psi_{gi} = -d\psi_{li} = \frac{W_i}{\sum_{j=1}^{K}\xi_j W_j} d\xi_{gi} = \frac{W_i A_i}{\sum_{j=1}^{K}\xi_j W_j} dp + \frac{W_i B_i}{\sum_{j=1}^{K}\xi_j W_j} dT \tag{18}$$

When a differential amount of heat per unit mass δq is added to the mixture at constant pressure,

$$dh = \xi_g(dh_g - dh_l) + dh_l + (h_g - h_l)d\xi_g = \delta q \tag{19}$$

The differential of enthalpy per unit mole for a multi-component gas or liquid is given as

$$dh = \left(\frac{\partial(h-h^*)}{\partial T}\,|_{p,X_i} + \frac{\partial h^*}{\partial T}\,|_{X_i}\right) dT + \sum_{i=1}^{K}\left(\frac{\partial(h-h^*)}{\partial X_i}\,|_{p,T,X_j,j\neq i} + \frac{\partial h^*}{\partial X_i}\,|_{T,X_j,j\neq i}\right) dX_i \tag{20}$$

Through Equations 19 and 20, the added heat δq causes a change dT in the temperature. The change in the temperature causes a shift in X_{gi}, X_{li}, ξ_{gi}, and ξ_{li} through Equations 17.
These equations can be used to consider a flow where methane and water flow together with two phases at the same temperature. One phase is a gas with methane and water vapor. The other phase has liquid water with dissolved methane. The above equations can be recast to give moles per unit volume (or mass per unit volume) and coupled with the energy equation. Results are expected over the next several months.

Zero-dimensional Model
In this model, composition and temperature vary with time but remain uniform in space. Pressure is constant and volume is allowed to change accordingly. Initial conditions must be provided. It is necessary that phase equilibrium is enforced in the initial state. Heat must be provided to drive the change of phase; combustion can occur only at higher temperatures where vaporization is completed. For this model, oxygen and fuel must be present in the initial state; they may enter through either phase or both phases.
From Equations 17, 18, 19, and 20, we may construct a system of ordinary differential equations governing the two-phase behavior as it proceeds through the shifting equilibrium change at constant pressure.

$$\frac{d\xi_{gi}}{dt} = -\frac{d\xi_{li}}{dt} = B_i\frac{dT}{dt}; \quad \frac{dX_{li}}{dt} = \left[\frac{X_{li}\sum_{j=1}^{K} B_j - B_i}{\xi_l}\right]\frac{dT}{dt}; \quad \frac{dX_{gi}}{dt} = \left[\frac{B_i - X_{gi}\sum_{j=1}^{K} B_j}{\xi_g}\right]\frac{dT}{dt}; i = 1, ..., K \tag{21}$$

The differentials for the fractional change $\dot{r}_i$ in gas mass of species i and for the fractional change $\dot{r}$ in total gas mass are given by

$$\dot{r}_i \equiv \frac{1}{\psi_g}\frac{d\psi_{gi}}{dt} = \frac{W_i B_i}{\sum_{j=1}^{K}\xi_{gj}W_j}\frac{dT}{dt}; \dot{r} \equiv \sum_{i=1}^{K} = \frac{1}{\psi_g}\frac{d\psi_g}{dt} = \frac{\sum_{i=1}^{K} W_i B_i}{\sum_{j=1}^{K}\xi_{gj}W_j}\frac{dT}{dt}; i = 1, ..., K \tag{22}$$

Now, the rate of enthalpy change can be related to the rate of heat addition (or subtraction) also to the time derivatives of temperature and mole fractions.

$$\frac{dh}{dt} = \psi_g\left(\frac{dh_g}{dt} - \frac{dh_l}{dt}\right) + \frac{dh_l}{dt} + (h_g - h_l)\frac{d\psi_g}{dt} = \frac{\delta q}{dt} = \dot{q} \tag{23}$$

The following relation can be applied for both the gas enthalpy h_g and the liquid enthalpy h_l.

$$\frac{dh}{dt} = \left(\frac{\partial(h-h^*)}{\partial T}|_{p,X_i} + \frac{\partial h^*}{\partial T}|_{X_i}\right)\frac{dT}{dt} + \sum_{i=1}^{K}\left(\frac{\partial(h-h^*)}{\partial X_i}|_{p,T,X_{j\neq i}} + \frac{\partial h^*}{\partial X_i}|_{T,X_{j\neq i}}\right)\frac{dX_i}{dt} \tag{24}$$

Substitution of Equation 24 into Equation 23 for the rates dh_g/dt and dh_l/dt yields a governing equation for the temperature derivative dT/dt. These first order ODEs are sufficient together with initial conditions to determine the $6K + 6$ variables $X_{gi}, X_{li}, \xi_{gi}, \xi_{li}, \psi_{gi}, \psi_{li}, \psi_g, \psi_l, h_g, h_l, h, T$ as functions of time during the heating and phase change at constant pressure.
Once the vaporization is completed or the mixture critical temperature has been exceeded, most of these equations have lost their usefulness; only Equation 24 would still be applicable for h_g. Since the heats of formation are included in h_g, that equation would still apply when gas-phase chemistry begins. It has been assumed however that

This work is licensed under a Creative Commons 4.0 International License (CC BY-NC-ND 4.0).
EDITORIAL UNIVERSITAT POLITÈCNICA DE VALÈNCIA

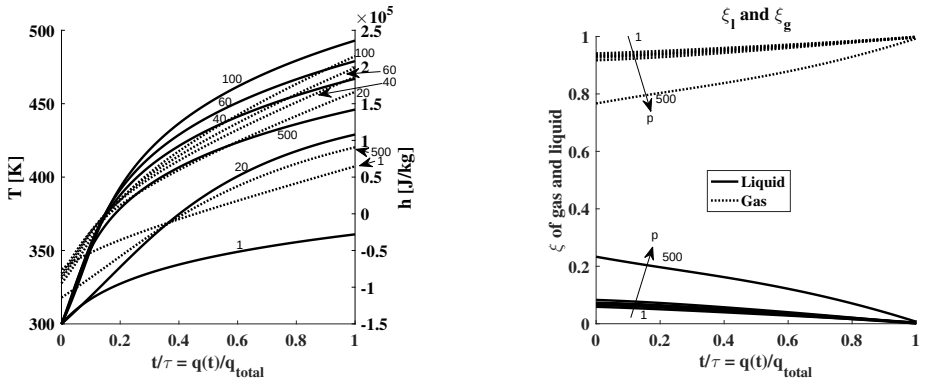

(a) Temperature and specific enthalpy

(b) Mole fraction of liquid and gas

Figure 6. (a) Temperature and specific enthalpy, (b) Mole fraction of liquid and gas, $p = [1 - 500]$ atm

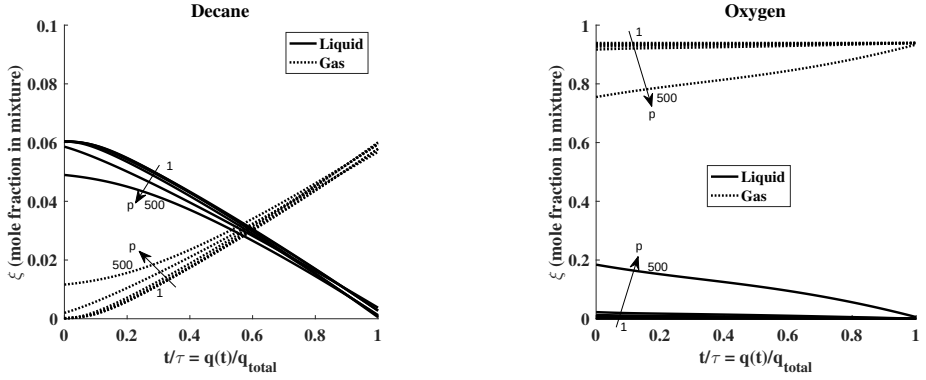

(a) Fraction of decane in mixture

(b) Fraction of oxygen

Figure 7. Mole fraction of species in mixture, $p = [1 - 500]$ atm

gas-phase chemistry begins after vaporization is completed or after the mixture critical temperature is exceeded. Once vaporization is completed, $h = h_g = constant$ and Equation 24 provides a relation between temperature change and composition change. Equations 21 and 22 no longer are relevant in the post-vaporization period; rather, changes in X_{gi}, ξ_{gi}, and ψ_{gi} will be driven by chemical kinetic laws.

Below are results for a binary mixture of decane and oxygen, which will be interesting to study both ignition and laminar flame problems. Results for a mixture of water and methane are not included for brevity, but they will also be discussed during the presentation. This second case relates directly to the methane-hydrate diffusion flames.

Let us consider 1 mole of decane and 15.5 moles of oxygen for a stoichiometric mixture between these two components. The mole fractions of each species in each phase are given from phase equilibrium at a given temperature and pressure.

The total number of moles in the liquid and in the gas are computed first. Then, ξ_g and ξ_l are obtained. In the following expression, subscript 1 stands for decane.

$$N_l = \frac{(\xi_1 - X_{g1})}{(X_{l1} - X_{g1})} N_0 \quad ; \quad N_g = N_0 - N_l \quad ; \quad \xi_l = \frac{N_l}{N_0} \quad ; \quad \xi_g = \frac{N_g}{N_0} \tag{25}$$

Finally, xi_{gi} and xi_{li} are calculated using Equation 11.

The horizontal axis in the following plots corresponds to the time t normalized by the heating time $\tau = q_{total}/(\delta q/dt)$, considering that heat is added at a constant rate. The values marked next to each curve are pressure magnitudes in [atm].

Figure 6a shows the evolution of temperature and mixture specific enthalpy from the beginning of the process (always at 300 K) until the liquid solution is completely vaporized, for pressures ranging from 1 to 500 atm. The difference between initial and final enthalpy represents the total heat added to vaporize all the liquid. This quantity increases with pressure from 1 to 100 atm, but the trend is inverted from 100 to 500 atm. Figure 6b shows the fractions of matter that belong to each phase as a function of the normalized time, for the various studied pressures. Because the considered mixture is composed predominantly of oxygen, the gas phase dominates initially. The liquid fraction is reduced almost linearly as heat is added and vaporization occurs. The fraction of liquid is greater for greater pressures, at any given instant throughout the process. The information in Figure 6b is dissected for the two species in Figures 7a and 7b. Liquid decane fraction decreases slower initially, and approximately after 25% of the process, it continues decreasing linearly. There is less liquid decane at higher pressures and more gaseous decane. The opposite effect occurs with oxygen, where more of it disolves into the liquid phase at higher

This work is licensed under a Creative Commons 4.0 International License (CC BY-NC-ND 4.0).
EDITORIAL UNIVERSITAT POLITÈCNICA DE VALÈNCIA

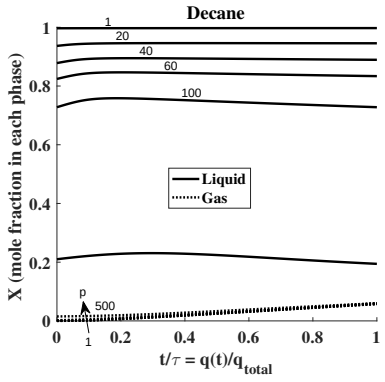

(a) Mole fraction of decane

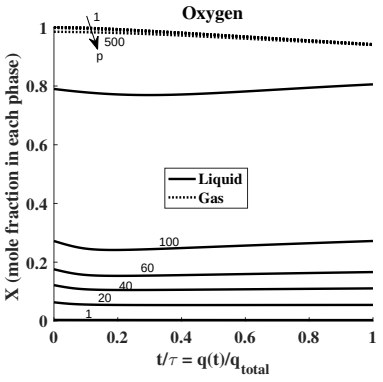

(b) Mole fraction of oxygen

Figure 8. Mole fraction of species, $p = [1 - 500]$ atm

pressures. Figures 8a and 8b show the mole fraction of each species in each phase throughout the whole process. The proportions of each species in the liquid phase are almost constant with time, except of slight variations at the beginning. For the gas phase, we see a slight monotonic increase in decane mole fraction while oxygen mole fraction is reduced.

Conclusions

Two-phase multicomponent mixtures are studied analytically and numerically using a cubic equation of state with appropriate high-density relations for enthalpies and potential functions at phase equilibrium. Results for vapor-liquid phase equilibrium are presented for binary mixtures of several hydrocarbons with oxygen and methane with water. These mixtures are relevant to practical situations in which a liquid is injected into a gas that is at supercritical conditions and for methane-hydrate combustion. Given this scenario, researchers usually assume single-phase behavior, while we show that two-phases exist at pressures that are several-fold the critical pressure of any single component within the mixture. Calculations are extended to mixtures with more than two components, where mole fraction ratios must be prescribed to close the system of equations.

A shifting equilibrium is considered as heat is added. Based on the shifting equilibrium assumption, a model for zero-dimensional, unsteady heating, vaporization, and exothermic reaction is presented. The one-dimensional, steady flow model is not presented for brevity. Nevertheless, together with the presented zero-dimensional model, it provides a template by which formulation can readily be made for a steady multidimensional model or unsteady models in one, two, or three dimensions. This would allow for the study of diffusion flames among other cases. The x-derivatives in the one-dimensional analysis can be replaced by gradient vector and divergence operators. Of course, boundary conditions will differ for diffusion flames but they are described in classical literature for single-phase behavior. The shifting equilibrium problem with decane and oxygen could be coupled with ignition delay or diffusion flame problems in future work. The case with a mixture of methane and water is interesting for methane-hydrate diffusion flames as well as for other applications where water is injected while being premixed with the fuel.

Acknowledgements

This research was supported by the NSF under Grant CBET-1333605 and AFOSR under Grant FA9550-15-1-0033. The first author appreciates the Balsells Fellowship support.

References

[1] J. P. Delplanque and W. A. Sirignano, "Transcritical vaporization and combustion of lox droplet arrays in a convective environment," *Combust. Sci. Technol.*, vol. 105, no. 4-6, pp. 327–344, 1995.

[2] S. M. Wallas, *Equilibria in Chemical Engineering*. Butterworth Pub., 1985.

[3] J. P. O,Connell and J. M. Haile, *Thermodynamics Fundamentals for Applications*. Cambridge University Press, 2005.

[4] G. Soave, "Equilibrium constants from a modified redlich-kwong equation of state," *Chem. Eng. Sci.*, vol. 27, pp. 1197–1203, 1972.

[5] G. Soave, S. Gamba, and L. A. Pellegrini, "Srk equation of state: Predicting binary interaction parameters of hydrocarbons and related compounds," *Fluid Phase Equilib.*, vol. 299, pp. 285–293, 2010.

[6] J. M. Prausnitz, R. N. Lichtenthaler, and E. G. de Azevedo, *Molecular Thermodynamics of Fluid-Phase Equilibria*. Englewood Cliffs, N.J.: Prentice Hall PTR, 1999.

[7] Y. V. C. Rao, *Chemical Engineering Thermodynamics*. Universities Press, 1997.

[8] B. E. Poling, J. M. Prausnitz, and J. P. O,Connell, *The Properties of Gases and Liquids, 5th Ed.* McGraw-Hill, 2001.

This work is licensed under a Creative Commons 4.0 International License (CC BY-NC-ND 4.0).
EDITORIAL UNIVERSITAT POLITÈCNICA DE VALÈNCIA